Breast Cancer Blood Flow and Metabolism on Dual-Acquisition ^{18}F-FDG PET: Correlation with Tumor Phenotype and Neoadjuvant Chemotherapy Response

Olivier Humbert[1,2], Maud Lasserre[2], Aurélie Bertaut[3], Pierre Fumoleau[4], Charles Coutant[5], François Brunotte[2,6,7], and Alexandre Cochet[2,6,7]

[1]Department of Nuclear Medicine, Centre Antoine-Lacassagne, Université Côte d'Azur, Nice, France; [2]Department of Nuclear Medicine, Centre G.F. Leclerc, Dijon, France; [3]Department of Biostatistics, Centre G.F. Leclerc, Dijon, France; [4]Department of Medical Oncology, Centre G.F. Leclerc, Dijon, France; [5]Department of Surgery, Centre G.F. Leclerc, Dijon, France; [6]Imaging Department, CHU Le Bocage, Dijon, France; and [7]Le2i FRE2005, CNRS, Arts et Métiers, Université Bourgogne Franche-Comté, Dijon, France

Early changes in tumor glucose metabolism (SUV_{max}) and in tumor blood flow (BF) have been evaluated separately for monitoring breast cancer response to neoadjuvant chemotherapy (NAC). This study used a single ^{18}F-FDG dual-acquisition PET examination to simultaneously assess these two imaging features and to determine whether they correlate with the same pretherapy tumor phenotypic features and whether they are comparable or complementary in predicting pathologic complete response (pCR). **Methods:** This prospective study included 150 women with breast cancer and an indication for NAC. A 2-min chest-centered dynamic PET acquisition was performed at the time of ^{18}F-FDG injection, followed by a delayed static PET acquisition 90 min later. Tumor BF was calculated from the dynamic acquisition using a validated first-pass model, and tumor SUV_{max} was calculated from the delayed acquisition. This dual acquisition was repeated after the first cycle of NAC to measure early changes in tumor BF and SUV_{max}. **Results:** A weak correlation was found between SUV_{max} and BF at baseline ($r = 0.22$; $P = 0.006$). A high baseline SUV_{max} was associated with all biologic markers of tumor aggressiveness, including the triple-negative breast cancer subtype ($P < 0.0001$). In contrast, a high baseline BF was associated only with obesity ($P = 0.002$). The change in SUV_{max} (mean, −44.6% ± 27.4%) varied depending on the Scarff–Bloom–Richardson grade, overexpression of human epidermal growth factor receptor 2 (HER2-positive), and lack of hormone receptor expression ($P = 0.04$, $P < 0.001$, and $P = 0.01$, respectively). BF (mean change, −26.9% ± 54.3%) showed a drastic reduction only in HER2-positive subtypes (−58.7% ± 30.0%), supporting the antiangiogenic effect of trastuzumab. Changes in SUV_{max} outperformed changes in BF for predicting pCR in all tumor subtypes: the areas under the curve for change in SUV_{max} were 0.82, 0.65, and 0.90 in the triple-negative, HER2-positive, and luminal subtypes, respectively. **Conclusion:** Of the two biologic hallmarks of cancer evaluated in this study, a reduction in tumor glucose metabolism was more accurate than a reduction in tumor BF for predicting pCR in the different subtypes of breast cancer.

Key Words: FDG PET; blood flow; metabolism; breast cancer; response

J Nucl Med 2018; 59:1035–1041
DOI: 10.2967/jnumed.117.203075

Neoadjuvant chemotherapy (NAC) is an approach used in breast cancer patients with a large primary tumor. The clinical benefit of NAC is that it increases the rate of breast-conserving surgery (*1*), but compared with conventional adjuvant chemotherapy, NAC does not improve patient outcomes (*1*). Nonetheless, studies have demonstrated that a pathologic complete response (pCR) at the end of NAC is an important surrogate marker of a favorable outcome (*2,3*). Thus, pCR has become a crucial endpoint in the neoadjuvant setting.

Angiogenesis and cell-energy deregulation are two hallmarks of oncogenesis (*4*). Both have been evaluated through different imaging modalities to assess tumor response to treatment in the neoadjuvant setting of breast cancer. Early changes in tumor glucose metabolism have been assessed mainly with ^{18}F-FDG PET (*5–7*), whereas changes in tumor blood flow (BF) have been assessed using various modalities, including dynamic contrast-enhanced MRI and ^{15}O-water PET.

In the neoadjuvant setting of breast cancer, treatment-related changes in tumor glucose metabolism (ΔSUV_{max}) have been reported to be a strong predictor of the pathologic response after the first or second cycle of NAC (*5–9*).

Different imaging modalities, such as dynamic contrast-enhanced MRI, ^{15}O-water PET, and 1-h dynamic ^{18}F-FDG PET, can yield kinetic parameters reflecting vascular permeability and perfusion. The quantification of tumor BF with these modalities has been reported to provide predictive and prognostic information while monitoring the effects of NAC (*10–15*). Because an on-site cyclotron in needed for ^{15}O-water PET studies, and because a full, 1-h, dynamic ^{18}F-FDG PET acquisition is hardly suitable in routine practice, there is a need to develop new analysis methods. To this end, Mullani et al. developed a 2-min dynamic first-pass PET acquisition based on a 1-compartment flow model to assess tumor BF (*16,17*).

The relationship and incremental value between the metabolic response and the response of tumor BF to NAC in breast cancer

Received Sep. 29, 2017; revision accepted Jan. 4, 2018.
For correspondence or reprints contact: Olivier Humbert, Centre Antoine Lacassagne, 33 Avenue de Valombrose, 06100 Nice, France.
E-mail: ohumbert@unice.fr
Published online Feb. 9, 2018.

TABLE 1
Patient Characteristics

Characteristic	*n*	%
Total patients	150	100
Age (y)		
≤50	80	53.3
50	70	46.7
Body mass index		
30	118	78.7
≥30	32	21.3
T stage		
T1–T2	128	85.3
T3–T4	22	14.7
Lymph node involvement		
No	58	38.7
Yes	92	61.3
Histologic type		
Ductal	139	92.7
Lobular	9	6
Other	2	1.3
SBR tumor grade		
Grade I	7	4.7
Grade II	65	43.3
Grade III	75	50
Unknown	3	2
SBR number of mitoses		
Score I	45	30
Score II	48	32
Score III	51	34
Unknown	6	4
Hormonal receptor status		
Negative	59	39.3
Positive	91	60.7
Tumor phenotype		
HER2	47	31.3
Luminal	61	40.7
TNBC	42	28
Surgery		
Mastectomy	61	40.7
Breast-conserving surgery	89	59.3
pCR		
ypT0/is		
Yes	42	28.0
No	108	72.0
ypN0		
Yes	93	72.0
No	57	38.0
ypT0/is ypN0		
Yes	39	26.0
No	111	74.0

SBR = Scarff–Bloom–Richardson grade.

has not yet been fully elucidated. By using a single ^{18}F-FDG dual-acquisition PET examination to assess both these image features, this study aimed to determine whether they correlate with the same pretherapy tumor phenotypes and whether they are comparable or complementary in predicting pCR.

MATERIALS AND METHODS

Patients and Study Design

From February 2009 to October 2014, women referred to the Centre G.F. Leclerc for clinical stage II or III biopsy-proven breast cancer with an indication for NAC were prospectively evaluated. This population overlaps those of previous articles published by our team (*8,9,17–20*). Patients with high glycemia (>9 mmol/L), those unwilling to undergo the complete PET examinations, and those with metastasis on the baseline ^{18}F-FDG PET were excluded. The institutional review board approved this prospective study as a current-care study. The medical team documented the nonopposition of the patient in source documents and on the information notice provided to the patient, and the need for a signature indicating informed consent was waived.

Tumor size and lymph node involvement were evaluated on ultrasonography. The women underwent various NAC regimens. Briefly, women with human epidermal growth factor receptor 2 (HER2)–positive tumors received trastuzumab and docetaxel-based regimens, and women with triple-negative or luminal/HER2-negative tumors received 6 cycles of sequential chemotherapy with anthracyclines and taxanes, or 6 cycles of FEC100 (epirubicin, 100 mg/m^2; 5-fluorouracil, 500 mg/m^2; and cyclophosphamide, 500 mg/m^2).

Within 1 mo after the last course of chemotherapy, the tumors were surgically removed. A pCR was defined as no residual invasive cancer in the breast or nodes, though in situ breast residuals were allowed (ypT0/is ypN0) (*3*).

^{18}F-FDG PET Procedures

A first ^{18}F-FDG PET scan was done at baseline (Gemini GXL and Gemini TF PET/CT scanners; Philips). The patients fasted for at least 6 h before intravenous injection of ^{18}F-FDG (5 MBq/kg for the Gemini GXL studies and 3 MBq/kg for the Gemini TF studies) using an automatic PET infusion system (Intego; Medrad) at a rate of 1 mL/s. Simultaneously with the injection, the first chest-centered emission acquisition with the patient prone, using a breast imaging coil, was run in list mode for 2 min, followed by a low-dose CT scan. Reconstructions of 5- and 10-s frames were extracted. Sixty minutes after the ^{18}F-FDG injection, a whole-body PET scan was done. Finally, 90 min after the injection, a PET scan restricted to the chest (2 bed positions) with the patient prone was performed.

A few days before the second course of chemotherapy, a second ^{18}F-FDG PET scan was performed with the same chest-restricted early dynamic first-pass acquisition and late (90 min) static acquisition.

BF Measurements. The concept and method of measuring tumor BF from the first pass of ^{18}F-FDG has been explained in a previous paper from our institution (*17*). It is based on the first-pass model of Mullani et al. described in previous reports (*16,21*). Volumes of interest encompassing the primary tumor and the ascending aorta were manually delineated using the 2-min dynamic summed functional and anatomic images. BF at baseline (BF1) and after the first cycle of chemotherapy (BF2) were then calculated in mL·min^{-1}·g^{-1} of tumor using the following equation (*16*):

$$\mathrm{BF} = \frac{Q(T_m)}{E \times \int_0^{T_m} Ca(t)dt \times V_t}.$$

$Q(T_m)$ is the amount of tracer in tumor tissue at time T_m measured with the tumor volume of interest. E is the tumor first-pass extraction

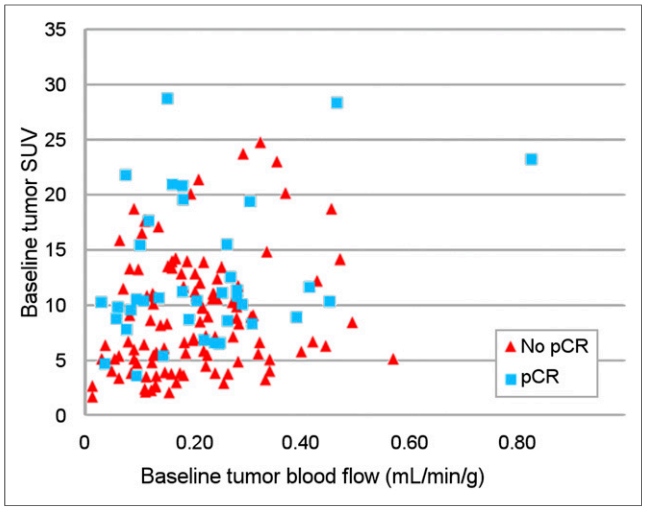

FIGURE 1. Correlation between BF1, SUV1, and pCR.

fraction of ^{18}F-FDG, which is assumed to equal 1 (*15*). $Ca(t)$ is the arterial concentration of the tracer at time t measured with the aorta volume of interest. V_t is the tumor volume (mL) delineated using the 2-min dynamic summed functional and anatomic images.

The BF response to chemotherapy (ΔBF) was calculated as

$$\Delta BF\,(\%) = 100 \times (BF2 - BF1)/BF1.$$

Tumor Glucose Metabolism Measurements. A spheroidal volume of interest encompassing the primary tumor was drawn on the 90-min chest-restricted acquisitions to measure the body-weight–corrected SUV_{max} at baseline ($SUV1_{max}$) and after the first course of chemotherapy ($SUV2_{max}$). The metabolic response (ΔSUV_{max}) in response to treatment was calculated as

$$\Delta SUV_{max}\,(\%) = 100 \times (SUV2_{max} - SUV1_{max})/SUV1_{max},$$

and the ratio between $SUV1_{max}$ and BF1 was calculated.

Statistical Analysis

Continuous variables were expressed as median with range or as mean with SD and were compared using either the Student test or nonparametric tests, depending on the normality of the distribution. Correlations between PET variables were determined using the Pearson correlation coefficient (r). Qualitative variables were expressed as percentages and compared using the χ^2 or Fisher test.

Receiver-operating-characteristic (ROC) curves were used to compare the predictive values of the different BF and SUV_{max} PET parameters for pCR. The areas under the curve (AUCs) were calculated with their 95% confidence intervals (95% CIs). A logistic regression model was also built to combine two different variables in ROC curve analyses. All analyses were performed using SAS software, version 9.4. The significance level was set at 0.05, except for multiple comparisons, which were handled using the Bonferroni adjustment (*22*).

RESULTS

Patient Characteristics

Table 1 details the characteristics of the 150 patients who were included. Median age was 49 y (range, 23–85 y). Median primary tumor size, assessed with breast ultrasonography or mammography, was 3.3 cm (range, 1.4–10 cm). The tumor subtype in most patients was luminal/HER2-negative (40.7%), followed by HER2-positive (31.3%) and triple-negative breast cancer (TNBC) (28%). pCR was achieved in 26% of the patients (39/150). The time from tracer injection to delayed breast acquisition was 84.8 ± 8.3 min (range, 68–112 min) on the baseline PET study and 85.6 ± 8.6 min (range, 66–110 min) on the interim PET study. The serum glucose level was 5.2 ± 0.7 mmol·L^{-1} (range, 2.9–7.6 mmol·L^{-1}) on the baseline PET study and 5.4 ± 0.9 mmol·L^{-1} (range, 3.8–9.4 mmol·L^{-1}) on the interim PET study.

Correlation Between $SUV1_{max}$, BF1, and Baseline Clinical/Histopathologic Parameters

A weak correlation was found between $SUV1_{max}$ and BF1 (r = 0.22; P = 0.006) (Fig. 1). Mean $SUV1_{max}$ was 10.2 (SD, 5.9), but the significance of the difference depended on the tumor subtype, with the highest significance observed in the TNBC subtype ($P < 1.10^{-4}$) (Table 2; Supplemental Fig. 1; supplemental materials are available at http://jnm.snmjournals.org). Mean BF1 was 0.21 mL·min^{-1}·g^{1} (SD, 0.13 mL·min^{-1}·g^{1}) and did not differ among breast cancer subtypes (P = 0.61) (Table 2).

After multiple-comparisons correction (n = 10, P cutoff = 0.005), a high $SUV1_{max}$ was significantly associated with the biologic markers of tumor aggressiveness: a high tumor grade (Scarff–Bloom–Richardson 3, $P < 0.001$), a negative hormone

TABLE 2
Tumor SUV_{max} and Tumor BF According to Breast Cancer Subtype

	HER2-positive	TNBC	Luminal/HER2-negative	P*
$SUV1_{max}$	9.5 ± 4.6	13. 9 ± 6.5	8.2 ± 5.2	<1.10^{-4}†
BF1 (mL·min^{-1}·g^{1})	0.20 ± 0.11	0.22 ± 0.10	0.21 ± 0.15	NS
$SUV1_{max}$/BF1	68.7 ± 66.3	79.2 ± 59.1	58.4 ± 52.5	0.011
ΔSUV_{max} (%)	−63.9 ± 20.1	−44.7 ± 27.1	−29.4 ± 23.0	<1.10^{-4}†
ΔBF (%)	−58.7 ± 30.2	−22.5 ± 51.2	−5.4 ± 59.6	1.10^{-4}†

*Kruskal–Wallis test.
†Statistically significant, using Bonferroni critical P value (multiple-comparisons corrections), calculated at 0.01.
NS = not significant.
Data are mean ± SD.

TABLE 3
Correlation Between Tumor PET Imaging Parameters and Histologic–Biologic Characteristics of Breast Cancer

Parameter	$SUV1_{max}$	$SUV2_{max}$	ΔSUV_{max}	BF1	BF2	ΔBF
SBR grade (I–II vs. III)	<0.001*	0.002*	0.040	NS	NS	NS
Body mass index (cutoff, 30)	NS	0.023	NS	0.002*	0.033	NS
Histologic type (ductal vs. lobular)	0.041	NS	NS	NS	NS	NS
HER2 overexpression (yes vs. no)	NS	<0.001*	<0.001	NS	<0.001*	<0.001*
HR status (positive vs. negative)	<0.001*	0.022	0.014	NS	NS	NS

*Statistically significant, using Bonferroni critical *P* value (multiple-comparisons corrections), calculated at 0.005.
SBR = Scarff–Bloom–Richardson grade; NS = not significant; HR = hormone receptor.
Data are *P* values obtained with Mann–Whitney test. Age, T stage, lymph node involvement, and menopausal status did not significantly correlate with tumor imaging characteristics.

receptor status ($P < 0.001$), and a high mitotic score ($P < 0.001$) (Table 3). In contrast, BF1 correlated with only body mass index (cutoff, 30): BF1 was 0.19 $mL \cdot min^{-1} \cdot g^1$ (SD, 0.12 $mL \cdot min^{-1} \cdot g^1$) in normal-weight women, versus 0.26 $mL \cdot min^{-1} \cdot g^1$ (SD = 0.12 $mL \cdot min^{-1} \cdot g^1$) in obese women ($P = 0.002$).

Response After First Cycle of NAC

Mean ΔSUV_{max} and ΔBF were −44.6% (SD, 27.4%) and −26.9% (SD, 54.3%), respectively. A moderate correlation was observed between ΔSUV_{max} and ΔBF ($r = 0.52$; $P < 0.001$) (Fig. 2). ΔSUV_{max} varied depending on Scarff–Bloom–Richardson grade, overexpression of human epidermal growth factor receptor 2 (HER2-positive), and lack of hormone receptor expression ($P = 0.04$, $P < 0.001$, and $P = 0.01$, respectively). But after multiple-comparisons correction, a higher ΔSUV_{max} and ΔBF were associated only with overexpression of HER2 ($P < 0.001$; Tables 2 and 3).

Pooled-Subtype Analysis. In the pooled analysis (Supplemental Table 1; Fig. 3; Supplemental Fig. 2) concerning SUV_{max}, ΔSUV_{max} was the best parameter to predict pCR, showing good diagnostic accuracy on ROC curve analysis (AUC, 0.82; 95% CI, 0.74–0.89; $P < 0.0001$). The pCR rate of patients with ΔSUV_{max} under or over the median percentage was 45.3% (34/75) and 6.7% (5/75), respectively ($P < 10^{-4}$). Concerning tumor BF, ΔBF was the best parameter to predict pCR but showed poor diagnostic accuracy on ROC curve analysis (AUC, 0.65; 95% CI, 0.55–0.74; $P = 0.003$). The pCR rate of patients with ΔBF under or over the median percentage was 32.0% (24/75) and 20.0% (15/75), respectively ($P = 0.09$). When ΔBF and ΔSUV_{max} were combined in ROC curve analysis, the predictive value was not improved over ΔSUV_{max} alone.

Per-Subtype Analysis. The per-subtype analysis (Supplemental Table 1; Fig. 3; Supplemental Fig. 2) showed that in triple-negative tumors, ΔSUV_{max} outperformed the other PET parameters in predicting pCR, with an AUC of 0.82 (95% CI, 0.68–0.95; $P < 0.0001$). $SUV2_{max}$ had a lower but still fair accuracy (AUC, 0.75; 95% CI, 0.59–0.91; $P = 0.003$). ΔBF and BF2 had worse accuracy (AUC, 0.66 and 0.68, respectively; $P = 0.05$ and 0.04, respectively). $SUV1_{max}$, BF1, and the $SUV1_{max}$/BF1 ratio failed to predict pCR (AUC < 0.60). The ROC curve analysis combining ΔBF and ΔSUV_{max} did not improve the AUC.

In patients with HER2-positive tumors, a high ΔSUV_{max} was predictive of pCR, with low accuracy (AUC, 0.66; $P = 0.05$). A low SUV2 had a low and insignificant accuracy (AUC, 0.65; $P = 0.09$). $SUV1_{max}$, BF1, BF2, ΔBF, and the $SUV1_{max}$/BF1 ratio failed to predict pCR (AUC < 0.60).

Among the 61 patients with luminal/HER2-negative cancer, only 3 achieved a pCR at the end of NAC. Despite this small number of pCRs, a high $SUV1_{max}$ and ΔSUV_{max} were both strong predictors of pCR, with excellent accuracies according to ROC curve analysis (AUC, 0.89 and 0.90, respectively; 95% CI = 0.73–1.00 and 0.69–1.00, respectively; $P < 0.0001$ for both). Only BF1 tended to predict pCR (AUC, 0.77; 95% CI, 0.49–1.00; $P = 0.06$); $SUV2_{max}$, BF2, ΔBF, and the $SUV1_{max}$/BF1 ratio did not. The ROC curve analysis combining ΔSUV_{max} and BF1 did not improve the AUC.

DISCUSSION

Functional imaging offers a unique opportunity to provide a noninvasive portrait of tumor biology. ^{18}F-FDG PET identifies patterns of tumor glucose metabolism and tumor BF that depend on the biologic characteristics of the breast cancer and the response to treatment.

The team from Seattle has also simultaneously quantified BF and tumor glucose metabolism using both ^{15}O-water PET and dynamic ^{18}F-FDG PET (*15,23–26*). Our BF1 values (0.21 vs.

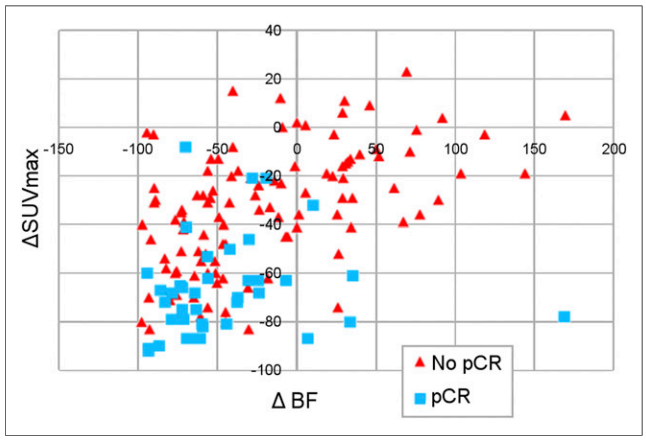

FIGURE 2. Correlation between early ΔBF, ΔSUV_{max}, and pCR.

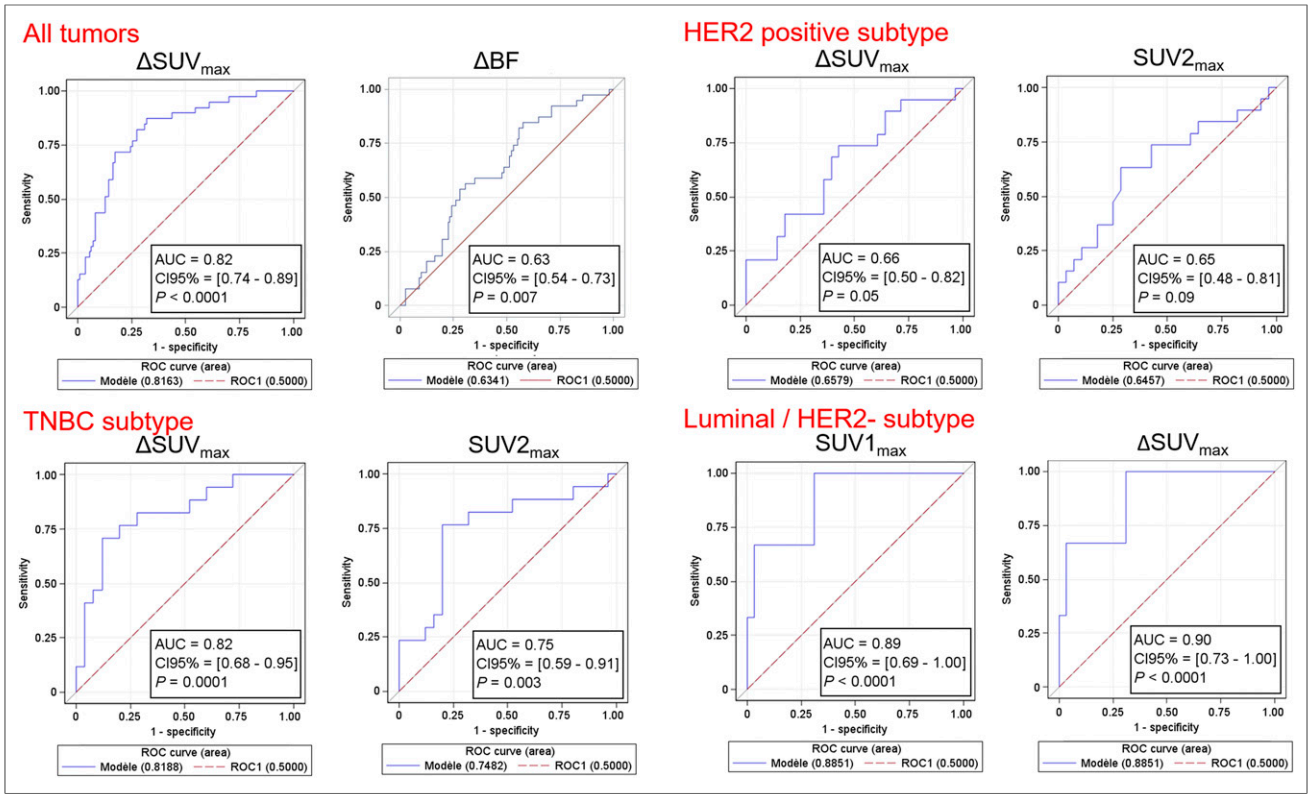

FIGURE 3. ROC curve analyses of best PET parameters for prediction of pCR, considering tumor subtype. CI95% = 95% confidence interval.

0.32 mL/min/g) and weak correlation between $SUV1_{max}$ and BF1 ($r = 0.22$ vs. 0.39) parallel their results (*25*).

As in previous reports, a high $SUV1_{max}$ correlated strongly with aggressive biologic characteristics, including the TNBC tumor subtype (*20,27*). In contrast, and in accord with the results of Dunnwald et al., we found no significant association between BF1 and the tumor phenotypic features and subtypes (*23*). BF1 was associated only with body mass index, with higher BF1 values being seen in obese women. Previous studies have underlined that obesity and adipose tissue dysfunction are linked to a proinflammatory and proangiogenic effect within the tumor microenvironment (*28,29*).

Specht et al. also demonstrated that an increased $SUV1_{max}$/BF1 ratio is associated with the TNBC subtype (*24*). It was hypothesized that this ratio reflects hypoxia. Using dual ^{18}F-FDG acquisitions, we also found that the $SUV1_{max}$/BF1 ratio was higher in women with the TNBC subtype.

After the first cycle of treatment, most tumors quickly exhibited significant decreases in both SUV_{max} and BF. But the correlation between these changes was rather weak. These 2 functional pathways may thus provide different and complementary biologic information. Moreover, as in previous studies, huge differences in response were observed among breast cancer subtypes (*7,20*). HER2-positive tumors are highly chemosensitive to trastuzumab and show a drastic drop in both SUV_{max} and BF after the first cycle of treatment. Contrary to the well-known high metabolic response, which correlates with the final pCR (*9*), the drastic drop in BF after the first cycle of trastuzumab has never, to our knowledge, been reported. This is an interesting finding because trastuzumab has been demonstrated to have a strong antiangiogenic effect (*30*). TNBC has been reported to show a good metabolic response, whereas response in luminal/HER2-negative tumors is lower (*20*). The present study revealed that the mean decrease in BF is low in both subtypes ($-22.5\% \pm 51.2\%$ for TNBC and $-2.7\% \pm 70.6\%$ for luminal/HER2-negative) and varies considerably depending on the tumor, suggesting biologic heterogeneity. The increase in BF observed in some tumors after the start of chemotherapy is an important issue. It may provide a valuable indication of tumor aggressiveness and chemoresistance, because an adequate blood supply is crucial to sustain rapid growth and metastasis (*31,32*). In a recent alternative hypothesis, the increase in BF in response to antiangiogenic drugs or phosphatidylinositol-3 kinase inhibitors was suggested to be a marker of treatment efficacy due to transient normalization of the abnormal tumor vasculature (*33*).

The aim of monitoring tumor response early during NAC is to predict final pCR and outcomes. Supporting our results, numerous studies have demonstrated that ^{18}F-FDG PET/CT accurately predicts the response to NAC in the HER2-positive and TNBC subtypes (*7,8*). Kinetic parameters linked to vascular permeability and perfusion have also been investigated in this setting, using different imaging modalities. For example, using sequential dynamic contrast-enhanced MRI, changes in pharmacodynamic parameters such as the AUC, the transfer constant, and the rate constant have been reported to be early predictors of a pCR to NAC (*10–12,34*). As another example, a ^{15}O-water PET study found that the $SUV1_{max}$/BF1 ratio correlated with the final pathologic response whereas BF1 did not (*25*). We found similar results using the dynamic ^{18}F-FDG first-pass model (Supplemental Table 1). In other studies, women with persistent or elevated BF on interim PET experienced worse tumor responses and outcomes (*15,26*).

Nonetheless, few studies have directly compared the BF and metabolic responses in the neoadjuvant setting of breast cancer (*35*). Tateishi et al. performed ^{18}F-FDG PET/CT and dynamic contrast-enhanced MRI at baseline and after 2 cycles of NAC, and PET/CT was more accurate in predicting a pCR (90.1% vs. 83.8% for ΔSUV_{max} and rate constant, respectively), but no per-subtype analyses were performed (*35*).

The main originality of the present study is that in a single ^{18}F-FDG PET examination, we combined a short, dynamic first-pass PET acquisition with a standard delayed PET acquisition, thus allowing direct comparison of the ability of early metabolic changes and blood flow changes to predict histologic response. In the analysis pooling all tumor subtypes, ΔBF predicted pCR, but its diagnostic accuracy on ROC curve analysis was lower than that of ΔSUV_{max} (AUC, 0.65 vs. 0.82, respectively). In the per-subtype analysis, metabolic parameters systematically outperformed BF in predicting pCR.

One limit of the study is that we did not determine its test–retest performance.

A PET biomarker predictive of tumor response may allow for early tailoring of the NAC regimen to an individual patient. The AVATAXHER phase 2 randomized trial has assessed the benefit of adding bevacizumab in women with poorly-responding HER2-positive tumors after 2 cycles of trastuzumab/docetaxel ($\Delta SUV_{max} <$ 70%) (*36*). No PET-guided therapeutic strategy has been evaluated in the TNBC subtype. In women with TNBC, the addition of bevacizumab increases the pCR rate but is also associated with higher rates of toxicities (*37*). The role of antiangiogenic drugs in the neoadjuvant setting should be further evaluated but limited to patients most likely to benefit, such as women with no BF response to a conventional NAC regimen.

CONCLUSION

Baseline tumor glucose metabolism correlated with the biologic markers of tumor aggressiveness, whereas baseline tumor BF correlated only with patient weight. Of these two hallmarks of cancer, the reduction in glucose metabolism was much more accurate in predicting pCR in the different subtypes of breast cancer. Randomized studies are needed to evaluate the clinical benefits of PET-based assessments in the early stages of NAC for breast cancer.

DISCLOSURE

No potential conflict of interest relevant to this article was reported.

ACKNOWLEDGMENT

We thank Philip Bastable for proofreading the manuscript.

REFERENCES

1. Mauri D, Pavlidis N, Ioannidis JPA. Neoadjuvant versus adjuvant systemic treatment in breast cancer: a meta-analysis. *J Natl Cancer Inst.* 2005;97:188–194.
2. Kuerer HM, Newman LA, Smith TL, et al. Clinical course of breast cancer patients with complete pathologic primary tumor and axillary lymph node response to doxorubicin-based neoadjuvant chemotherapy. *J Clin Oncol.* 1999;17:460–469.
3. von Minckwitz G, Untch M, Blohmer J-U, et al. Definition and impact of pathologic complete response on prognosis after neoadjuvant chemotherapy in various intrinsic breast cancer subtypes. *J Clin Oncol.* 2012;30:1796–1804.
4. Hanahan D, Weinberg RA. Hallmarks of cancer: the next generation. *Cell.* 2011;144:646–674.
5. Rousseau C, Devillers A, Sagan C, et al. Monitoring of early response to neoadjuvant chemotherapy in stage II and III breast cancer by [^{18}F]fluorodeoxyglucose positron emission tomography. *J Clin Oncol.* 2006;24:5366–5372.
6. Avril S, Muzic RF, Plecha D, Traughber BJ, Vinayak S, Avril N. ^{18}F-FDG PET/CT for monitoring of treatment response in breast cancer. *J Nucl Med.* 2016;57 (suppl 1):34S–39S.
7. Groheux D, Mankoff D, Espié M, Hindié E. ^{18}F-FDG PET/CT in the early prediction of pathological response in aggressive subtypes of breast cancer: review of the literature and recommendations for use in clinical trials. *Eur J Nucl Med Mol Imaging.* 2016;43:983–993.
8. Humbert O, Riedinger J-M, Charon-Barra C, et al. Identification of biomarkers including ^{18}FDG-PET/CT for early prediction of response to neoadjuvant chemotherapy in triple-negative breast cancer. *Clin Cancer Res.* 2015;21:5460–5468.
9. Humbert O, Cochet A, Riedinger J-M, et al. HER2-positive breast cancer: ^{18}F-FDG PET for early prediction of response to trastuzumab plus taxane-based neoadjuvant chemotherapy. *Eur J Nucl Med Mol Imaging.* 2014;41:1525–1533.
10. Ah-See M-LW, Makris A, Taylor NJ, et al. Early changes in functional dynamic magnetic resonance imaging predict for pathologic response to neoadjuvant chemotherapy in primary breast cancer. *Clin Cancer Res.* 2008;14:6580–6589.
11. Johansen R, Jensen LR, Rydland J, et al. Predicting survival and early clinical response to primary chemotherapy for patients with locally advanced breast cancer using DCE-MRI. *J Magn Reson Imaging.* 2009;29:1300–1307.
12. Sun Y-S, He Y-J, Li J, et al. Predictive value of DCE-MRI for early evaluation of pathological complete response to neoadjuvant chemotherapy in resectable primary breast cancer: a single-center prospective study. *Breast.* 2016;30:80–86.
13. Tseng J, Dunnwald LK, Schubert EK, et al. ^{18}F-FDG kinetics in locally advanced breast cancer: correlation with tumor blood flow and changes in response to neoadjuvant chemotherapy. *J Nucl Med.* 2004;45:1829–1837.
14. Zasadny KR, Tatsumi M, Wahl RL. FDG metabolism and uptake versus blood flow in women with untreated primary breast cancers. *Eur J Nucl Med Mol Imaging.* 2003;30:274–280.
15. Dunnwald LK, Gralow JR, Ellis GK, et al. Tumor metabolism and blood flow changes by positron emission tomography: relation to survival in patients treated with neoadjuvant chemotherapy for locally advanced breast cancer. *J Clin Oncol.* 2008;26:4449–4457.
16. Mullani NA, Herbst RS, O'Neil RG, Gould KL, Barron BJ, Abbruzzese JL. Tumor blood flow measured by PET dynamic imaging of first-pass ^{18}F-FDG uptake: a comparison with ^{15}O-labeled water-measured blood flow. *J Nucl Med.* 2008;49:517–523.
17. Cochet A, Pigeonnat S, Khoury B, et al. Evaluation of breast tumor blood flow with dynamic first-pass ^{18}F-FDG PET/CT: comparison with angiogenesis markers and prognostic factors. *J Nucl Med.* 2012;53:512–520.
18. Humbert O, Berriolo-Riedinger A, Cochet A, et al. Prognostic relevance at 5 years of the early monitoring of neoadjuvant chemotherapy using ^{18}F-FDG PET in luminal HER2-negative breast cancer. *Eur J Nucl Med Mol Imaging.* 2014;41:416–427.
19. Humbert O, Riedinger J-M, Vrigneaud J-M, et al. ^{18}F-FDG PET-derived tumor blood flow changes after 1 cycle of neoadjuvant chemotherapy predicts outcome in triple-negative breast cancer. *J Nucl Med.* 2016;57:1707–1712.
20. Humbert O, Berriolo-Riedinger A, Riedinger JM, et al. Changes in ^{18}F-FDG tumor metabolism after a first course of neoadjuvant chemotherapy in breast cancer: influence of tumor subtypes. *Ann Oncol.* 2012;23:2572–2577.
21. Mullani NA, Goldstein RA, Gould KL, et al. Myocardial perfusion with rubidium-82. I. Measurement of extraction fraction and flow with external detectors. *J Nucl Med.* 1983;24:898–906.
22. Neuhäuser M. How to deal with multiple endpoints in clinical trials. *Fundam Clin Pharmacol.* 2006;20:515–523.
23. Dunnwald LK, Doot RK, Specht JM, et al. PET tumor metabolism in locally advanced breast cancer patients undergoing neoadjuvant chemotherapy: value of static versus kinetic measures of fluorodeoxyglucose uptake. *Clin Cancer Res.* 2011;17:2400–2409.
24. Specht JM, Kurland BF, Montgomery SK, et al. Tumor metabolism and blood flow as assessed by positron emission tomography varies by tumor subtype in locally advanced breast cancer. *Clin Cancer Res.* 2010;16:2803–2810.
25. Mankoff DA, Dunnwald LK, Gralow JR, et al. Blood flow and metabolism in locally advanced breast cancer: relationship to response to therapy. *J Nucl Med.* 2002;43:500–509.

26. Mankoff DA, Dunnwald LK, Gralow JR, et al. Changes in blood flow and metabolism in locally advanced breast cancer treated with neoadjuvant chemotherapy. *J Nucl Med.* 2003;44:1806–1814.
27. Gil-Rendo A, Martínez-Regueira F, Zornoza G, García-Velloso MJ, Beorlegui C, Rodriguez-Spiteri N. Association between [^{18}F]fluorodeoxyglucose uptake and prognostic parameters in breast cancer. *Br J Surg.* 2009;96:166–170.
28. Mantovani A, Allavena P, Sica A, Balkwill F. Cancer-related inflammation. *Nature.* 2008;454:436–444.
29. Iyengar NM, Gucalp A, Dannenberg AJ, Hudis CA. Obesity and cancer mechanisms: tumor microenvironment and inflammation. *J Clin Oncol.* 2016;34:4270–4276.
30. Izumi Y, Xu L, di Tomaso E, Fukumura D, Jain RK. Tumour biology: Herceptin acts as an anti-angiogenic cocktail. *Nature.* 2002;416:279–280.
31. Carmeliet P, Jain RK. Angiogenesis in cancer and other diseases. *Nature.* 2000;407:249–257.
32. Carmeliet P. Angiogenesis in life, disease and medicine. *Nature.* 2005;438:932–936.
33. Carmeliet P, Jain RK. Principles and mechanisms of vessel normalization for cancer and other angiogenic diseases. *Nat Rev Drug Discov.* 2011;10:417–427.
34. Choi WJ, Kim WK, Shin HJ, Cha JH, Chae EY, Kim HH. Evaluation of the tumor response after neoadjuvant chemotherapy in breast cancer patients: correlation between dynamic contrast-enhanced magnetic resonance imaging and pathologic tumor cellularity. *Clin Breast Cancer.* 2018;18:e115–e121.
35. Tateishi U, Miyake M, Nagaoka T, et al. Neoadjuvant chemotherapy in breast cancer: prediction of pathologic response with PET/CT and dynamic contrast-enhanced MR imaging—prospective assessment. *Radiology.* 2012;263:53–63.
36. Coudert B, Pierga J-Y, Mouret-Reynier M-A, et al. Use of [^{18}F]-FDG PET to predict response to neoadjuvant trastuzumab and docetaxel in patients with HER2-positive breast cancer, and addition of bevacizumab to neoadjuvant trastuzumab and docetaxel in [^{18}F]-FDG PET-predicted non-responders (AVATAXHER): an open-label, randomised phase 2 trial. *Lancet Oncol.* 2014;15:1493–1502.
37. Sikov WM, Berry DA, Perou CM, et al. Impact of the addition of carboplatin and/or bevacizumab to neoadjuvant once-per-week paclitaxel followed by dose-dense doxorubicin and cyclophosphamide on pathologic complete response rates in stage II to III triple-negative breast cancer: CALGB 40603 (Alliance). *J Clin Oncol.* 2015;33:13–21.